PALEOCEANOGRAPHY, VOL. 22, PA3211, doi:10.1029/2006PA001394, 2007

Warm upwelling regions in the Pliocene warm period

Petra S. Dekens,[1] Ana Christina Ravelo,[1] and Matthew D. McCarthy[1]

Received 17 November 2006; revised 16 February 2007; accepted 26 March 2007; published 10 August 2007.

[1] Given the importance of upwelling processes to coastal productivity and regional climate, it is critical to study the role of upwelling regions within the context of global climate change. We generated sea surface temperature (SST) records for the last 5 million years in three important upwelling regions: the eastern equatorial Pacific, the California margin, and the Peru margin. Prior to ~3.0 Ma, SSTs at all sites were significantly warmer than today (by 3–9°C), indicating that cold upwelling regions that characterize the modern Pacific Ocean did not exist in the early Pliocene warm period (4.6 to 3.1 Ma), Earth's most recent period of sustained global warmth. Alkenone, phosphorus, and organic carbon mass accumulation rate records indicate that changes in productivity and SST were decoupled and that upwelling of nutrient enriched water occurred even when SSTs were warm during the early Pliocene. Thus the long-term trends in SST are likely explained by changes in the temperature of upwelled water rather than in the strength of upwelling-favorable winds alone. The fact that gradual cooling of upwelling regions began before the onset of significant Northern Hemisphere glaciation provides further evidence that the growth of ice sheets and their influence on atmospheric winds alone can not explain the cooling of upwelling regions. Our results suggest that the long-term average SSTs of upwelling regions are influenced by global changes in the depth and/or temperature of the ventilated thermocline.

Citation: Dekens, P. S., A. C. Ravelo, and M. D. McCarthy (2007), Warm upwelling regions in the Pliocene warm period, *Paleoceanography*, *22*, PA3211, doi:10.1029/2006PA001394.

1. Introduction

[2] Upwelling regions are key features of the modern climate. Along eastern boundaries of ocean basins, cool nutrient-rich subsurface water upwells to the surface, supporting diverse ecosystems of continental margins that are biologically productive and important in the global carbon cycle [*Lampitt et al.*, 1995]. The cool sea surface temperatures (SST) contribute to globally important air-sea interactions [*Seager et al.*, 2003; *Lau and Shen*, 1988] that influence regional climate [*Seager et al.*, 2003]. Given the central role of upwelling regions in regulating regional and basin scale climate and coastal productivity, an important challenge in current climate research is to understand the response of upwelling systems to global warming trends. Global warming could result in increased upwelling favorable winds [*Bakun*, 1990; *Snyder et al.*, 2003], as has been observed over the last several decades [*Mendelssohn and Schwing*, 2002]. However, because the thermocline along the California margin has deepened at the same time, recent increases in physical upwelling have been accompanied by increasing SST [*Mendelssohn and Schwing*, 2002] and decreasing zooplankton productivity [*Roemmich and McGowan*, 1995]. This apparent decoupling between winds and SST within the relatively short instrumental record highlights the need for geological studies that explore the role and response of upwelling systems to long term climate change, particularly during times of global warmth.

[1]Ocean Sciences Department, University of California, Santa Cruz, California, USA.

0883-8305/07/2006PA001394$12.00

[3] We focus on upwelling regions in the Pacific Ocean (Figure 1) during the early Pliocene (4.6 to 3.1 Ma), a period of global warmth, and the transition to the Pleistocene, a globally cooler time with larger amplitude glacial-interglacial cycles. While not a perfect analog for an anthropogenically warmed Earth, the early Pliocene period is the most recent time in Earth's history when long-term mean climate was warmer than today (3°C warmer on average) and when boundary conditions (e.g., position of continents, major ocean currents, Northern Hemisphere ice sheet size, and atmospheric pCO_2) were similar to the present [*Ravelo et al.*, 2004]. Global climate change of the last 5 Ma includes the end of the early Pliocene warm period, global cooling, and the onset of significant Northern Hemisphere glaciation (NHG) (Figure 2).

[4] The most complete record of SST changes in an upwelling region over the last 4.5 Ma comes from the west coast of Africa (at ODP site 1084), where early Pliocene SST was 10°C warmer than present, and decreased as global climate cooled and Northern Hemisphere ice sheets grew [*Marlow et al.*, 2000]. An increase in the percent of upwelling diatoms from 4.5 Ma to the present indicates a gradual increase in upwelling from the Pliocene to the Pleistocene. The researchers hypothesize that the onset of NHG increased the pole to equator temperature gradient, thereby increasing upwelling favorable winds. An alternative explanation for warmer SST in upwelling regions during the early Pliocene, prior to NHG, calls on changes in the temperature of the source of upwelling water, which can be controlled by changes in the depth of the thermocline [*Fedorov et al.*, 2004, 2006]. As the Earth's climate cooled through the Cenozoic, the thermocline may have gradually shoaled due to changes in extratropical conditions which

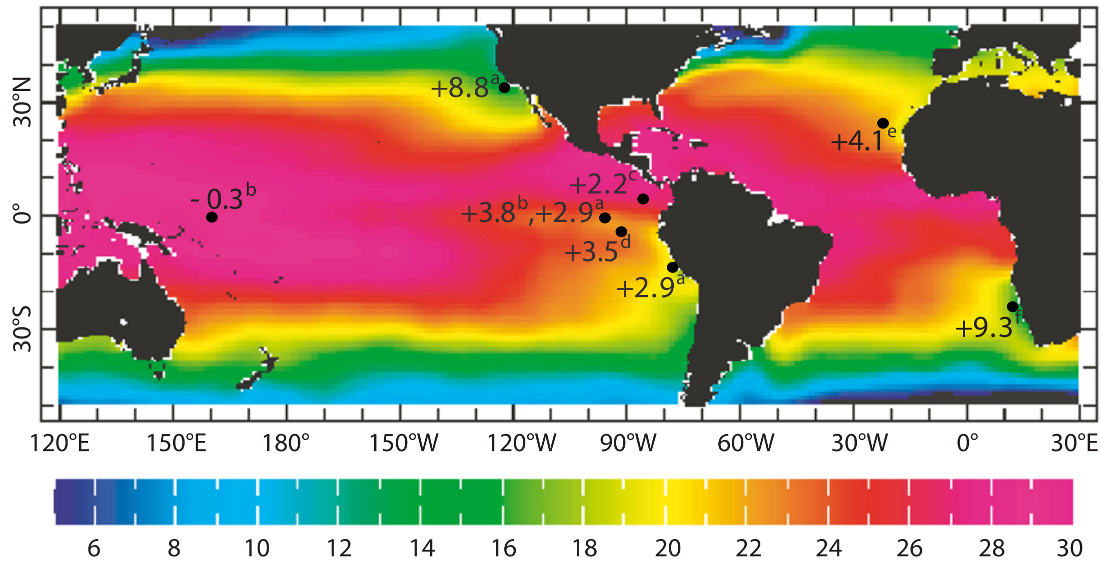

Figure 1. Difference in sea surface temperature (SST) between Pliocene and modern SST. The colored map shows modern mean annual SST [*Levitus and Boyer*, 1994]. Superimposed is the difference between the average Pliocene SST (3–4.6 Ma) minus the modern mean annual SST for (a) three $U^{k'}_{37}$ records in this study (+8.8°C, +2.9°C, +2.9°C for Ocean Drilling Project (ODP) site 1014 in the California margin, ODP site 847 in the east equatorial Pacific (EEP), and ODP site 1237 in the Peru margin, respectively), (b) Mg/Ca records at ODP site 847 in the EEP and ODP site 806 in the west equatorial Pacific (WEP) [*Wara et al.*, 2005], (c) a Mg/Ca record at ODP site 1241 in the EEP [*Groeneveld et al.*, 2006] (shown at paleobacktrack location and compared to modern SST at that location, due to possible influence of northward plate movement on SST), (d) a $U^{k'}_{37}$ record at ODP site 846 [*Lawrence et al.*, 2006], (e) a $U^{k'}_{37}$ record at ODP site 958 in the eastern equatorial Atlantic [*Herbert and Schuffert*, 1998], and (f) a $U^{k'}_{37}$ record at ODP site 1084 in the Benguela current [*Marlow et al.*, 2000].

determine its depth [e.g., *Fedorov et al.*, 2004], reaching a critical depth ~3 Ma when cool water within or below the thermocline was shallow enough to be mixed to the surface by winds [*Federov et al.*, 2006; *Philander and Fedorov*, 2003].

[5] In this study we generated SST records spanning the last 5 m.y. in the California margin, Peru margin, and the east equatorial Pacific (EEP) upwelling regions, using the alkenone unsaturation index ($U^{k'}_{37}$) as a proxy for SST. Along with the SST estimates, we present new C_{37} mass accumulation rate (MAR) records and published paleoproductivity proxy records as indicators of productivity at these locations. By comparing trends in SST with those in paleoproductivity and by considering the timing of SST changes relative to the ice volume record, we consider the possible mechanisms that could have led to changes in SSTs through the Pliocene and Pleistocene.

2. Background

[6] In the EEP cold water from below the thermocline is brought to the surface through equatorial divergent upwelling caused by the trade winds, while in the northeast and southeast Pacific coastal upwelling is caused by the equatorward winds of the subtropical high-pressure systems. During "normal" conditions in the modern tropical Pacific, easterly trade winds result in a thick warm mixed layer and a deep thermocline (>200 m) in the western equatorial Pacific (WEP) and a shallow thermocline in the EEP (~50 m). Trade winds cause divergent upwelling all along the equator, but, due to the tilt of the thermocline, warm water from above the thermocline upwells in the WEP, while cool nutrient rich water from below the thermocline upwells to the surface in the EEP. This results in a SST (Figure 1) and sea level pressure (SLP) gradient along the equator. The SLP gradient in turn strengthens the trade winds, which further increases the SST and SLP gradients [*Cane*, 1986]. The atmospheric circulation, including the easterly trade winds, low SLP and rising air in the WEP, westerly winds aloft, and high SLP and sinking air in the EEP, is referred to as Walker circulation [*Cane*, 1986]. During an El Niño event the trade winds weaken or disappear, and the tilt of the thermocline and SST gradient across the Pacific decreases, resulting in warmer SST and lower SLP in the EEP [*Cane*, 1986].

[7] Along the eastern boundaries of the northeast and southeast Pacific, alongshore equatorward winds and offshore Ekman pumping driven by cyclonic wind stress curl result in offshore transport of surface water and vertical transport of cool nutrient enriched water from below the relatively shallow thermocline to the surface [*Bakun and Nelson*, 1991]. The equatorward winds are influenced by the strength and position of the subtropical high-pressure systems, which respond to changes in the pole to equator temperature gradient [*Rind*, 1998]; the wind strength increases (decreases) as the pole to equator temperature

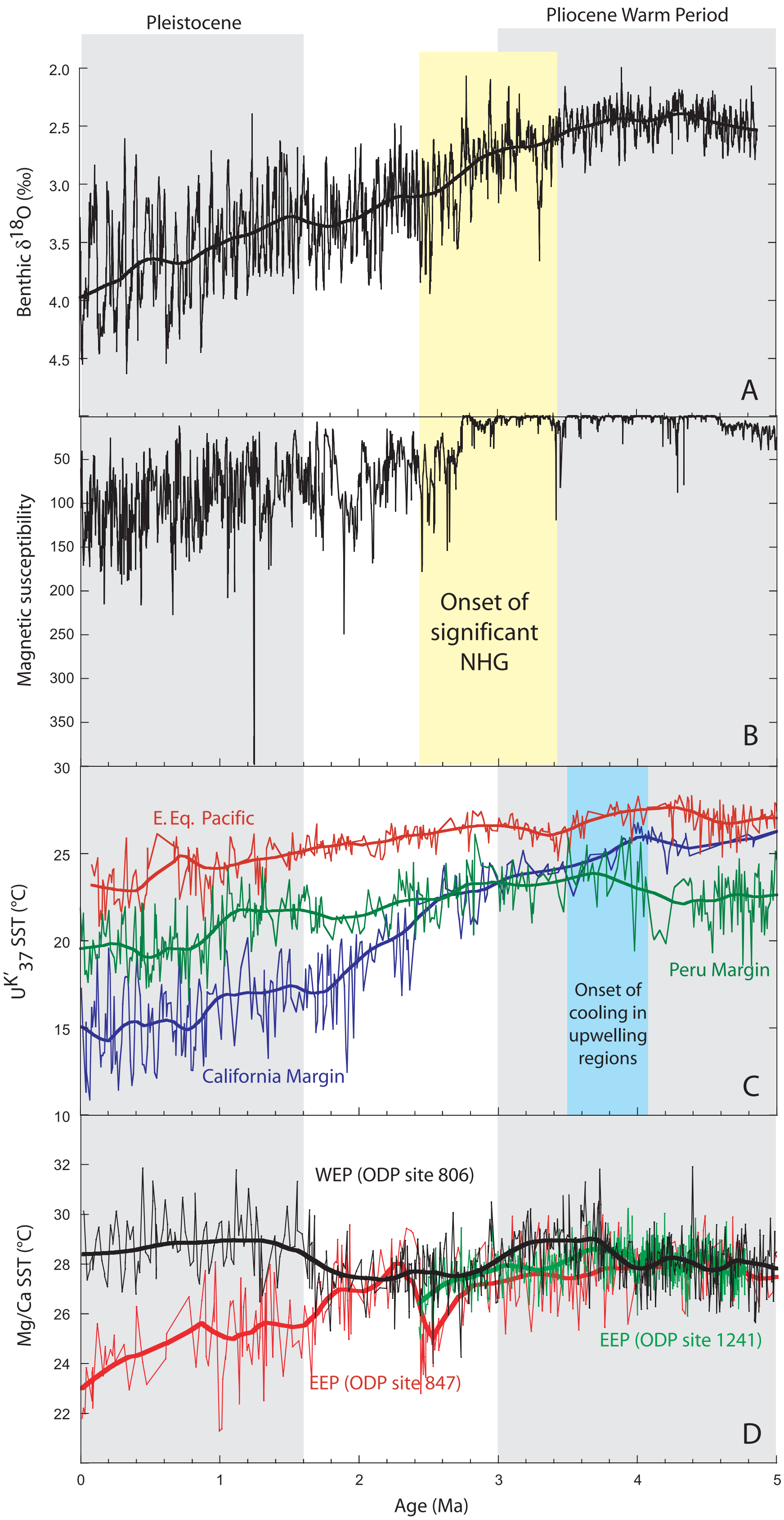

Pleistocene
Pliocene Warm Period
Benthic δ18O (‰)
A
Magnetic susceptibility
Onset of significant NHG
B
E. Eq. Pacific
Peru Margin
California Margin
Onset of cooling in upwelling regions
UK'37 SST (°C)
C
WEP (ODP site 806)
EEP (ODP site 1241)
EEP (ODP site 847)
Mg/Ca SST (°C)
D
Age (Ma)

Figure 2

gradient increases (decreases). The winds also vary seasonally; summertime heating of the continents and the development of strong low-pressure conditions over land strengthens the Pacific subtropical high-pressure system, resulting in stronger upwelling-favorable winds and cool SSTs [*Bakun*, 1990]. The strength of the high-pressure systems is also influenced by SLP in the WEP; rising air from the WEP low-pressure system flows aloft to the east as part of Walker circulation but also flows toward subtropical high-pressure systems as part of Hadley circulation. During an El Niño event the weakening low-pressure system in the WEP results in weaker subtropical high-pressure systems, reduced upwelling favorable winds along the California and Peru margins [*Schwing et al.*, 2002], and increased SST in these upwelling locations. In sum, the strength of the subtropical high, and therefore of upwelling favorable winds in the eastern Pacific Ocean, are influenced by three main factors: the pole to equator temperature gradient, seasonal monsoonal heating of the continents, and SLP in the WEP.

[8] Mechanisms that explain changes in SST in upwelling regions include not only those that involve atmospheric circulation and winds but also those that involve oceanic processes that impact the subsurface water. Upwelling can lead to warm SST where the thermocline is deep, as described above for the WEP. Thus changes in SST may be influenced by changes in the depth of the thermocline. For example, in the California current, the increase in upwelling over the past few decades has led to higher SST rather than lower SST as might be expected because the thermocline along the California margin has been depressed causing warm mixed layer water rather than cold water from below the thermocline to upwell [*Mendelssohn and Schwing*, 2002].

[9] The depth of the global thermocline is controlled by two main processes: deep thermohaline circulation and shallow wind-driven circulation of the ventilated thermocline [*Boccaletti et al.*, 2004]. Cold water sinking at high latitudes as part of thermohaline circulation fills the ocean basins and is heated by the diffusion of heat from warm surface water throughout the world's oceans [*Bryan*, 1987]. The relative importance of thermohaline circulation and the ventilated thermocline in driving the depth of the global thermocline depends on the diffusivity of the ocean. If diffusivity is low, as suggested by observations of low mixing in the thermocline [*Ledwell et al.*, 1993], then wind driven circulation and the ventilated thermocline become the dominant processes balancing the ocean heat budget [*Boccaletti et al.*, 2004]. Cool surface water from extratropical regions is subducted to a few hundred meters and travels within the ventilated thermocline along subsurface isopycnals, eventually making its way to upwelling regions where winds force this cool water to the surface [*Philander and Fedorov*, 2003]. In order to balance the ocean heat budget, ocean heat lost at middle and high latitudes must equal the heat gained in cold upwelling regions [*Boccaletti et al.*, 2004; *Fedorov et al.*, 2004; *Philander and Fedorov*, 2003]. For example, if anthropogenic climate change leads to more warming at high latitudes compared to low latitudes, the ocean heat flux to the atmosphere at high latitudes would be reduced, and the thermocline heat budget would be balanced by a deepening of the thermocline, reducing the heat gained in upwelling regions [*Federov et al.*, 2006]. Such a change would eventually cause warmer SSTs in regions of upwelling.

3. Methods

[10] Age models were determined using shipboard biostratigraphic ages for Ocean Drilling Program (ODP) Site 1237 [*Mix et al.*, 2003] (16°S, 76°23′W, 3212 m water depth), using GRAPE tuned age model for ODP Site 847 [*Shackleton et al.*, 1995] (0°12′N, 95°19′W, 3334 m water depth), and using an oxygen isotope and magnetic susceptibility tuned age model for ODP Site 1014 [*Ravelo et al.*, 2004] (32°50′N, 119°59′W, 1165 m water depth). Sampling resolution ranges from 10 to 20 kyr.

[11] Separation and quantification of alkenones were performed at the University of California Santa Cruz. Total organics were separated from 0.25 to 0.75 g of sediment using a methylene chloride and methanol (in a 3:1 ratio) solution in three sonication and extraction iterations. The solvent was pushed through a 1 μm pore size PTFE filter to remove any residual sediment, dried under a nitrogen stream, and redissolved in 50–250 μL of toluene spiked with hexatriacontane and heptatriacontane as internal standards. Then 1 μL was injected into a Hewlett-Packard 6890 GC equipped with a flame ionization detector in the splitless mode (purge flow 30 mL/min for 2 min). Separation of $C_{37:2}$ and $C_{37:3}$ alkenones was achieved using a 60 m DB-1 column with a 0.30 mm internal diameter and 0.1 μm film thickness. A deactivated fused silica guard column was clipped ~15 cm daily, and the 4 mm gooseneck inlet liner was replaced ~2/week to maintain good chromatography. The initial oven temperature was 90°C, while the inlet temperature was maintained at 300°C throughout. The oven temperature program used was temperature increased by 25°C/min until 250°C, increased by 1°C/min until 303°C, increased by 20°C/min to 330°C, and held for 20 min. The

Figure 2. Pliocene-Pleistocene climate records from different regions. (a) Benthic foraminifera δ^{18}O record of high-latitude climate change [*Ravelo and Andreasen*, 2000; *Shackleton et al.*, 1990]. (b) Magnetic susceptibility from ODP site 882 [*Haug et al.*, 1999]. (c) $U_{37}^{k'}$ SST records from ODP site 847 in the EEP (red), ODP site 1237 in the Peru margin (green), and ODP site 1014 in the California margin (blue). Thin lines connect individual data points, while thicker lines are weighted smoothing curves. (d) Mg/Ca SST at ODP site 806 in the WEP (black) and ODP site 847 in the EEP (red) [*Wara et al.*, 2005], and Mg/Ca SST at ODP site 1241 [*Groeneveld et al.*, 2006] indicating the establishment of strong Walker circulation at ~2 Ma. All Mg/Ca records were generated utilizing *G. sacculifer* (without sac-like final chamber) and converted to temperature using the carbonate ion corrected calibration of *Dekens et al.* [2002].

Table 1. Comparison of Pliocene and Modern SST[a]

ODP Site	Location	Modern SST	Pleistocene Avg (0–0.5 Ma)	Pliocene Avg (3–4.6 Ma)	Difference Plio-Pleistocene	Difference Pliocene - Modern	Reference
1014	California Margin	15.9°C	15.1 ± 2.3°C	24.7 ± 1.1°C	9.6°C	8.8°C	this study
1237	Peru Margin	20.0°C	19.6 ± 1.4°C	22.9 ± 1.5°C	3.3°C	2.9°C	this study
847	EEP	23.9°C	23.0 ± 1.2°C	26.8 ± 0.4°C	3.8°C	2.9°C	this study
847	EEP	23.9°C	23.8 ± 1.1°C	27.7 ± 1.2°C	3.9	3.8°C	*Wara et al.* [2005]
846	EEP	22.5°C	22.2 ± 1.0°C	26.0 ± 0.8°C	3.8	3.5°C	*Lawrence et al.* [2006]
1241	EEP	26.0°C	NA	28.2 ± 0.7°C	NA	2.2°C	*Groeneveld et al.* [2006]
806	WEP	29.1°C	29.5 ± 1.2°C	29.4 ± 1.0°C	−0.1°C	−0.3°C	*Wara et al.* [2005]
928	East Atlantic	21.5°C	NA	25.6 ± 0.8°C	NA	4.1°C	*Herbert and Schuffert* [1998]
1084	Benguela Current	16.5	14.8 ± 2.0°C	25.8 ± 0.9°C	11°C	9.3°C	*Marlow et al.* [2000]

[a]Columns from left to right are site number, site location, modern annual average SST [*Levitus and Boyer*, 1994], averaged Pleistocene $U^{k'}_{37}$ SST using all data from 0 to 0.5 Ma, averaged Pliocene SST using all data from 3 to 4.6 Ma, the difference between averaged Pliocene and Pleistocene $U^{k'}_{37}$, the difference between averaged Pliocene SST and modern annual average SST. Note that for site 1241 the modern SST is for the site's backtracked Pliocene location because of the potential influence that northward plate movement had on the SST record at this site.

unsaturation index was calculated as $U^{k'}_{37} = C_{37:2}/(C_{37:2} + C_{37:3})$ [*Prahl et al.*, 1988].

[12] Instrument precision is based on replicates of our lab liquid consistency standard, which is an extract from ODP site 1014. Four replicates of the consistency standard were analyzed with each run and long term instrument precision is ±0.005 for $U^{k'}_{37}$, equivalent to ±0.14°C. The precision of the entire method, including the extraction procedure, is based on replicates of ODP site 847 and ODP site 1014 sediment standards. One sediment standard was processed with each set of samples. Long-term precision is ±0.01 (±0.35°C) and ±0.008 (±0.24°C) for ODP site 847 and ODP site 1014 sediment standards, respectively. For quantification of alkenone concentrations, instrument precision is 25%, and the external precision is 35%. No correlation was found between the amount of alkenones injected and the temperature estimate.

4. Results

[13] Alkenones are long-chain ethyl and methyl ketones that vary in the number of double bonds between carbon atoms and are produced by a small number of coccolithophorids [*Volkman*, 2000]. The degree of unsaturation of the 37 carbon ketones (as recorded by the $U^{k'}_{37}$ index) is related to the growth temperature of the algae that produce them. We measured $U^{k'}_{37}$ in sediments from ODP site 847 in the EEP, ODP Site 1014 in the California margin, and ODP Site 1237 in the Peru margin (Figure 1), and converted $U^{k'}_{37}$ values to SST using a global calibration [*Müller et al.*, 1998].

[14] The California margin cooled ~3°C from 4.5 to 2.5 Ma, followed by a more dramatic cooling of 6°C from 2.5 to 1.5 Ma (Figure 2c). The Peru margin warmed slightly between 5 and 4 Ma, then cooled by ~2°C from 4 to 1 Ma, and cooled another ~1.5°C from 1 Ma to present (Figure 2c). The EEP cooled gradually from ~4.5 Ma to the present (Figure 2c). Although the cooling in the EEP and the Peru margin was not as dramatic as that in the California margin, the dominant feature of these two records is the gradual ~3°C cooling that begins at ~4 Ma, continues through the onset of significant NHG, to the late Pleistocene. All three records show a cooling trend between 4 and 3 Ma (~2.5°C at the California margin and ~1.3°C in the EEP and Peru margins), before the onset of significant NHG (Figure 2). At all three sites, average SST approached modern interglacial values by ~2 Ma. The records indicate that SST variability was highest in the late Pleistocene (Figure 2), consistent with high amplitude glacial-interglacial cycles, as reflected in the global ice volume (δ^{18}O) record (Figure 2a).

[15] Average SST during the early Pliocene (3–4.6 Ma) was substantially warmer compared to the late Pleistocene (0–0.5 Ma) and modern mean annual SST (Table 1) at each site. The California margin SST was 9.6°C warmer during the Pliocene compared to the late Pleistocene and 8.8°C warmer than modern mean annual SST (Figure 1 and Table 1). The EEP and the Peru margin show comparable SST change; the Pliocene was 3.8°C and 3.3°C warmer than the late Pleistocene, respectively, and 2.9°C warmer than modern mean annual SST at both locations (Figure 1 and Table 1). Our $U^{k'}_{37}$ SST estimates at ODP site 1237 are consistent with a low-resolution record at the same site [*Abe et al.*, 2006].

[16] The alkenone mass accumulation rate (MAR) at the California margin was much higher than at the EEP and Peru Margin throughout the records and shows a period of high coccolithophorid productivity from ~1.5 to 3 Ma (Figure 3a). Alkenone MAR in the EEP shows a similar peak in productivity from ~1.5 to 3 Ma (Figure 3b), but there is more variability throughout the record. The alkenone MAR at the Peru margin shows a peak in coccolithophorid productivity from ~0.2 to 1 Ma (Figure 3c).

5. Discussion

[17] $U^{k'}_{37}$ has become a widely used paleo-SST proxy in part because the organic C_{37} alkenones are extremely well preserved in sediments [*Harvey*, 2000; *Prahl et al.*, 1989], making them resistant to dissolution issues that affect many other proxies. While changes in the dominant species, depth

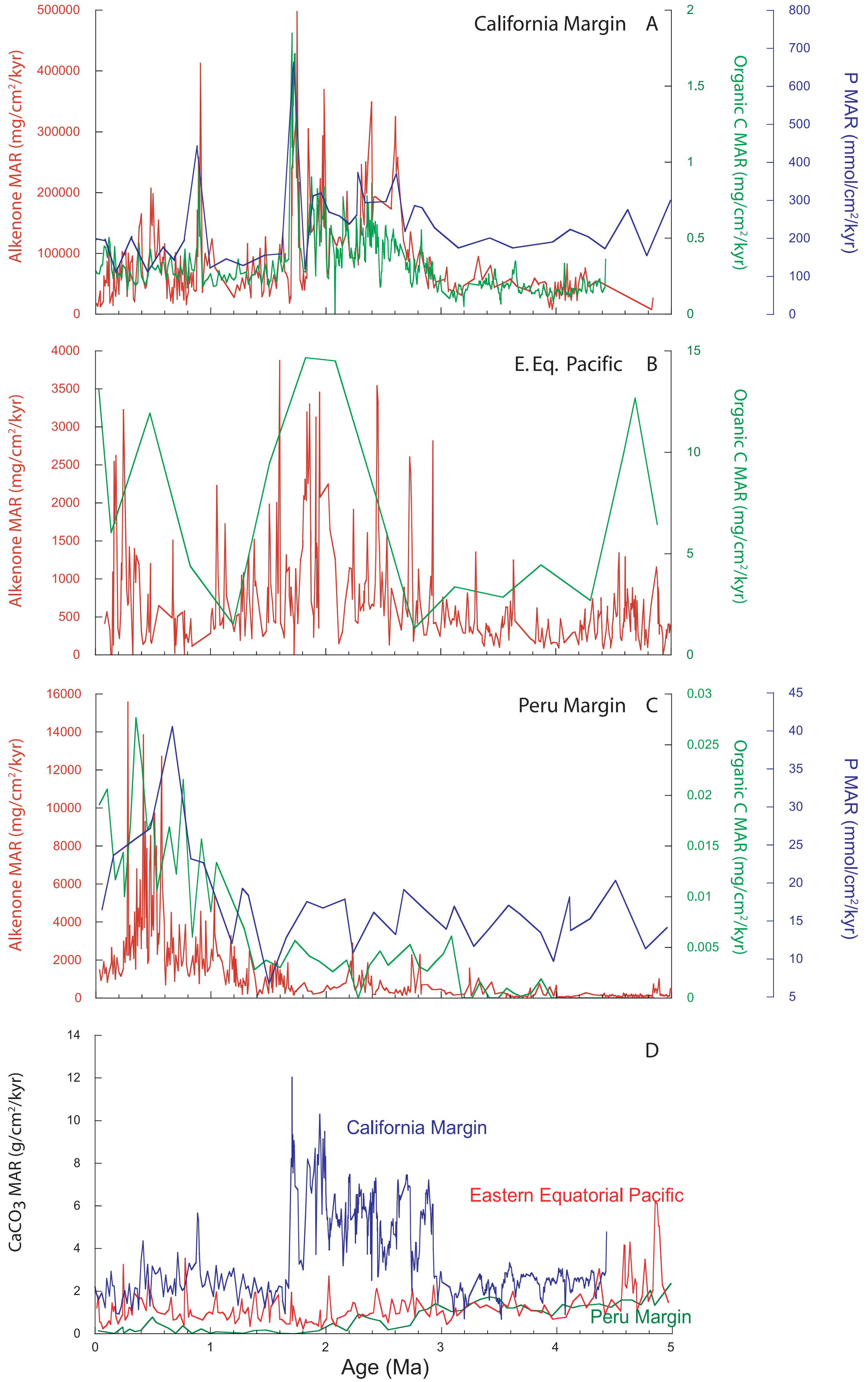
California Margin A
Alkenone MAR (mg/cm²/kyr)
Organic C MAR (mg/cm²/kyr)
P MAR (mmol/cm²/kyr)
E. Eq. Pacific B
Peru Margin C
D
CaCO3 MAR (g/cm²/kyr)
California Margin
Eastern Equatorial Pacific
Peru Margin
Age (Ma)

Figure 3

ecology, and/or seasonality of alkenone producing algal species can potentially influence $U_{37}^{k'}$ records, there is no evidence that our SST records are substantially biased by these factors. Trends in our SST records are not associated with changes in the dominant species of nanoplankton [*Lyle et al.*, 1997; *Mayer et al.*, 1992; *Mix et al.*, 2003] consistent with previous work [*Villaneuva et al.*, 2002]. The cooling trend in our $U_{37}^{k'}$ SST record in the EEP (Figure 2c) is similar to the trend in a Mg/Ca SST record at the same site (Figure 2d) [*Wara et al.*, 2005] but different from that in a record of subsurface water temperatures (not shown) [*Wara et al.*, 2005], demonstrating that $U_{37}^{k'}$ is not substantially biased by subsurface production of alkenones. Because coccolithophorids tend to proliferate under well-stratified, nonupwelling conditions [*Okada and Honjo*, 1973], $U_{37}^{k'}$ could record seasonal nonupwelling conditions rather than mean annual SST. The increase in seasonal upwelling through the Pliocene along the California margin [*Ravelo et al.*, 2004] would tend to minimize the SST changes (as recorded by $U_{37}^{k'}$) and therefore can not explain the large cooling trend in our California margin $U_{37}^{k'}$ record since the warm Pliocene. Finally, the similarity between the Mg/Ca of *G. sacculifer* (P. S. Dekens et al., A 5 million year comparision of the Mg/Ca and alkenone paleo-thermometers, manuscript in preparation, 2007) (a species of foraminifera which grows year round) (Figure 2d) and our $U_{37}^{k'}$ record in the EEP demonstrates that seasonal bias in our $U_{37}^{k'}$ record is minimal.

[18] Our $U_{37}^{k'}$ SST record at ODP site 847 in the EEP, together with other SST records in the EEP cold tongue [*Wara et al.*, 2005; *Lawrence et al.*, 2006] and the WEP warm pool [*Wara et al.*, 2005], indicate an El Niño-like pattern of SST in the tropical Pacific during the warm Pliocene (Figure 1) as suggested previously [*Ravelo et al.*, 2006, and references therein]. The reduced east-west SST gradient in the Pliocene is mostly a result of warmer SST in the EEP, as the WEP SST changes little [*Wara et al.*, 2005]. A new *G. sacculifer* Mg/Ca record at ODP site 1241, just north of the equatorial cold tongue, was interpreted to be inconsistent with an El Niño-like pattern because the early Pliocene Mg/Ca temperature estimates at this site are similar to (rather than warmer than) modern mean annual temperatures at 30 m [*Groeneveld et al.*, 2006]. However, this interpretation rests on the selection of a calibration [*Nürnberg et al.*, 2000] based on cultured *G. sacculifer.* The resulting early Pliocene SST estimates were cooler than three other data sets indicating warmer SST in the EEP: $U_{37}^{k'}$ SST data at ODP Site 847 (this study), $U_{37}^{k'}$ SST data at ODP Site 846 [*Lawrence et al.*, 2006], and Mg/Ca SST data at ODP Site 847 [*Wara et al.*, 2005] in which the *Dekens et al.* [2002] calibration was used. To eliminate Mg/Ca-SST calibration issues, it is useful to compare the average early Pliocene (3–4.6 Ma) Mg/Ca values of *G. sacculifer* at ODP site 1241 (3.26 mmol/mol) [*Groeneveld et al.*, 2006], at ODP site 847 (3.06 mmol/mol) [*Wara et al.*, 2005], and at ODP site 806 (3.54 mmol/mol) [*Wara et al.*, 2005] to illustrate that Mg/Ca values were nearly the same at both EEP sites and at the WEP site. Hence contrary to the interpretation presented by *Groeneveld et al.* [2006], the ODP site 1241 Mg/Ca data is in fact consistent with a reduced west-east SST gradient during the early Pliocene. To calculate SST from Mg/Ca data, it makes most sense to use the same calibration at all sites. We convert Mg/Ca to SST using the *Dekens et al.* [2002] calibration because it is based on analyses of *G. sacculifer* from coretops in the tropical Pacific, takes into account possible dissolution effects on the Mg/Ca composition of foraminiferal calcite, and yields the most realistic SST for Pleistocene interglacials at ODP sites 847 and 806 (to our knowledge, no Pleistocene data is available at ODP site 1241) (Figure 2d). The resulting pattern of Pliocene SST in the EEP, expressed as a difference relative to modern mean annual SST (Figure 1), with most warming in the equatorial cold tongue ($\sim$3–4°C) and less warming north of the cold tongue (2°C), is consistent with an El Niño-like pattern of SST.

[19] Our three $U_{37}^{k'}$ records indicate warmer than modern SST in Pacific upwelling regions during the early Pliocene. One possible explanation, discussed first, is that there was less intense upwelling due to weaker winds. Winds could have been weaker in the Pliocene, prior to the onset of NHG, due to the reduced equator to pole temperature gradient [*Dowsett et al.*, 1996; *Marlow et al.*, 2000]. Weaker winds could also have resulted from atmospheric teleconnections from the tropical Pacific. Specifically, warm Pliocene El Niño-like conditions, including reduced Walker circulation [*Wara et al.*, 2005], must have been accompanied by a less intense low pressure region in the WEP, which could have resulted in weaker subtropical high pressure zones [*Schwing et al.*, 2002] and reduced upwelling-favorable winds in the California and Peru margins.

[20] Cooling SSTs and a gradual increase in upwelling through the Pliocene-Pleistocene in the Benguela Current was hypothesized to be related to the onset of NHG and the associated strengthened winds due to the larger pole to equator temperature gradient [*Marlow et al.*, 2000]. However, upwelling regions in the Pacific Ocean began cooling at $\sim$4 Ma, prior to the onset of significant NHG as recorded by $\delta^{18}O$ (3.6 to 2.4 Ma) [*Mudelsee and Raymo*, 2005] and ice rafted debris (2.75 Ma) (Figure 2) [*Haug et al.*, 1999]. Thus if there was a change in the strength of upwelling favorable winds, the fact that upwelling SSTs began cooling before the

Figure 3. (a) C_{37}, organic carbon, and phosphorous mass accumulation rates (MAR). Alkenone MAR, organic carbon MAR [*Lyle et al.*, 1997], and phosphorus MAR [*Delaney and Anderson*, 2000] for ODP site 1014 in the California margin. (b) Alkenone MAR and organic carbon MAR [*Mayer et al.*, 1992] for ODP site 847 in the EEP. (c) Alkenone MAR, organic carbon MAR [*Mix et al.*, 2003], and phosphorus MAR [*Chun and Delaney*, 2006] for ODP site 1237 in the Peru margin. (d) $CaCO_3$ MAR for ODP site 1014 in the California margin (blue) [*Ravelo et al.*, 2004], ODP site 847 in the EEP (red) [*Farrell et al.*, 1995], and ODP site 1237 [*Mix et al.*, 2003].

onset of NHG indicates that the growth of the ice sheets and the resulting changes in atmospheric winds alone can not explain the cooling of all upwelling regions. Any changes in wind strength are therefore more likely related to teleconnections with the tropical Pacific as conditions shifted from a permanent El Niño-like pattern in the early Pliocene, to a La Niña-like pattern with a strong low-pressure zone over the WEP warm pool and enhanced subtropical high-pressure systems in the Pleistocene.

[21] If SST changes were related to changes in wind strength alone we would expect a strong correlation between SST and productivity, since physical upwelling vertically transports nutrient rich water from the subsurface. Alkenone (C_{37}), organic carbon (C_{org}), and phosphorus mass accumulation rates (MAR) provide a first-order qualitative indication of productivity. In the California margin, the C_{37}, C_{org}, and phosphorus MAR are relatively high from ∼1.5 to 3 Ma (Figure 3a). This pattern is also seen in $CaCO_3$ MAR at this site (Figure 3d), indicating the peak in C_{37} is due to higher productivity of coccolithophorids, rather than preservation changes [*Ravelo et al.*, 2004]. The EEP shows a similar peak in C_{37} and C_{org} MAR from ∼1.5 to 3 Ma (Figure 3b), consistent with results from a nearby site (ODP site 846), which also indicate relatively high C_{37} total and % organic carbon during this time interval, and point to high levels of productivity [*Lawrence et al.*, 2006]. The $CaCO_3$ MAR (Figure 3d) record in the EEP is different than the paleoproductivity records discussed, with a maximum MAR before 4 Ma, due to changes in preservation of calcite at this location [*Farrell et al.*, 1995]. Overall, at the California margin and in the EEP, changes in productivity are not correlated to changes in SST.

[22] In contrast, at the Peru margin all three paleoproductivity indicators show higher MAR from 1.5 Ma to the present (Figure 3c). Thus unlike the records from the California margin and the EEP discussed above, there was probably an increase in productivity in the Pleistocene as SSTs cooled. However, tectonic movement of ODP site 1237 site from the open ocean toward the coastal zone of intense productivity through the last 5 Ma could account for part of this trend. Similarly, the modern pattern of SST in this region indicates that the movement of the site could also account for a small portion of the SST trend at this site (<1°C) [*Mix et al.*, 2003]. Tectonic movements of ODP sites 1014 and 847 would not have appreciably affected SST trends at these locations.

[23] The inverse relationship between SST and productivity that would be expected if SST changes were related to wind driven upwelling alone is observed only in the Peru margin and not in the EEP or California margin. A more direct indicator of upwelling, such as the prevalence of upwelling diatoms used in the Benguala current [*Marlow et al.*, 2000], should be applied in future work to further define changes in biophysical processes at our locations. However, the productivity indicators used here show a consistent pattern and demonstrate that in the EEP and the California margin over the last 5 Ma SST and total productivity are decoupled, and relatively high productivity was sustained even when SSTs in upwelling regions were warm in the Pliocene. This suggests that our SST records are unlikely to be the result of changes in wind strength alone; rather SSTs in these upwelling regions were likely influenced by fundamental changes in the conditions in the subsurface ocean, which is the source of upwelled waters.

[24] Warmer SST in upwelling regions in the early Pliocene, and cooling SST through time, could involve changes in the depth of the global thermocline. It is possible that during the warm Pliocene the thermocline was deeper and/or its steepness was reduced, as has been observed in the equatorial Pacific [*Wara et al.*, 2005; *Chaisson and Ravelo*, 2000]. Relatively warm upwelling regions in the early Pliocene are also found in the Atlantic (Figure 1) [*Marlow et al.*, 2000; *Herbert and Schuffert*, 1998], lending further support that the Atlantic and Pacific regions could have been similarly influenced by altered (warmer and/or deeper) thermocline conditions which caused warm, rather than cool water, to upwell to the surface [*Federov et al.*, 2006]. Our observations that productivity and SST changes were decoupled indicate that oceanic processes that altered thermocline conditions globally were probably largely independent from those that influenced subsurface nutrient distributions. For the early Pliocene, this idea explains why relatively warm SST in upwelling regions globally occurred at the same time that there was relatively high productivity and suggests that subsurface water was warm but nutrient-enriched. Change in the source of upwelling water has been documented in the Benguela current; the abundance of diatom species associated with a Southern Ocean source of water was at a maximum from ∼1.9 to 3.2 Ma, indicating that the source of upwelling water may have been Antarctic Intermediate Water, rather than the South Atlantic Central Water which is upwelled in this region today [*Marlow et al.*, 2000]. Overall, there is preliminary evidence that the cooling of upwelling regions through the Pliocene was not only related to increased wind-driven upwelling, but much work is needed to understand the interplay between changes in the sources of upwelled water, ecosystem evolution, and cooling of upwelling regions through the Pliocene.

[25] While it is clear that a shallower thermocline could explain the cooling of upwelling regions, the cause of the thermocline shoaling through the Pliocene and Pleistocene is unclear. Three processes could have played a role: (1) the closing of the Panama Seaway, (2) the restriction of the Indonesian Seaway, and (3) changes in surface ocean conditions and poleward heat transport. The hypothesis that the closing of the Panama seaway is the direct cause of the onset of significant NHG has been put into question due to the difference in timing between the closing of the seaway and NHG [*Mudelsee and Raymo*, 2005], as well as model results that indicate an enhanced Gulf Stream Current would have warmed SST in high latitudes and hindered the buildup of ice sheets [*Klocker et al.*, 2004]. However, it is clear that the closing of the Panama seaway influenced intermediate water: the relative flux of North Atlantic intermediate water (NAIW) probably increased when the seaway closed [*Haug and Tiedemann*, 1998]. The northward movement of New Guinea and the restriction of the Indonesian Seaway is

another tectonic process which could impact thermocline conditions [*Cane and Molnar*, 2001]. When New Guinea was further south than its modern position, subsurface water last ventilated in the North Pacific was returned in the equatorial undercurrent while South Pacific water (saltier and warmer than equivalent density water from the North Pacific) moved into the Indian Ocean via the seaway; opposite to modern conditions. The change in source water to the equatorial undercurrent has been hypothesized to be the cause of the El Niño-like pattern in SST in the tropical Pacific [*Cane and Molnar*, 2001].

[26] While the closing of the Panama Seaway could have caused changes in the thermocline in the Atlantic Ocean, and the restriction of the Indonesian Seaway could have caused changes in the thermocline structure of the Pacific and Indian Oceans, it is unclear how either would have caused changes in the global thermocline. Perhaps a more likely scenario is that the reduced equator to pole temperature gradient in the early Pliocene led to a more locally balanced heat budget, resulting in a deeper ventilated thermocline [*Boccaletti et al.*, 2004; *Federov et al.*, 2006; *Philander and Fedorov*, 2003]. More evidence for a globally shoaling thermocline could come from subsurface temperature records. Changes in the depth of the ventilated thermocline should yield similar subsurface temperature histories globally, with warmer subsurface temperatures when the thermocline was deep in the Pliocene, followed by cooling subsurface temperatures as the thermocline shoaled.

6. Implications

[27] While our data provide strong proof that the SSTs of today's eastern Pacific cold upwelling regions were warmer in the early Pliocene, the implications of this observation on global and regional climate of the early Pliocene are many and require continued investigation. In this section, we introduce some of the possible climatic impacts of warm upwelling regions; specifically, we discuss how they may have been related to the global warmth of the early Pliocene and the suppression of North American ice sheet growth and how they may have impacted regional climate conditions.

[28] One important consequence of globally warmer upwelling regions is that these conditions may have contributed to the global warmth of the early Pliocene through their impact on the albedo and/or the greenhouse gas, water vapor. If the warm upwelling regions were themselves a result of high-latitude warmth, then upwelling regions (through their impact on albedo and water vapor) would have been part of a feedback loop that amplified global warming. To begin to test this idea, a modeling study was conducted [*Barreiro et al.*, 2005], in which the response of climate to the absence of zonal SST gradients (from 40°S to 30°N) was calculated. The study shows that the absence of cold upwelling regions alone can cause global warming of about 0.5°C to >2.0°C depending on the seasonality and mean low-latitude temperature [*Barreiro et al.*, 2005]. The global warming is mainly due to reduced highly reflective stratus clouds (and reduced albedo) and increased water vapor content of the atmosphere, both caused by warmer than modern temperatures in upwelling region.

[29] Warm upwelling regions potentially had a strong impact on the suppression of Northern Hemisphere glaciation in the early Pliocene. In the modeling experiments of *Barreiro et al.* [2005], the absence of cold upwelling regions and zonal SST gradients resulted in strong warming in some regions at certain times of year through teleconnections; for example, >5°C warmer than modern conditions on the North American continent during winter (but not the summer). In more recent times (the late Quaternary), wintertime temperatures in the continental interior were cold enough for snow to fall and accumulate, and thus North American ice sheet size has been critically dependent on summer temperature [*Pollard*, 2000], which controls ablation rates. In contrast, during the early Pliocene, wintertime temperature in the North American continental interior may have been warm enough that perennial snowfall was suppressed, thereby exerting some control on ice sheet growth. North American warmth would have been maintained by warm upwelling and permanent El Niño-like conditions through teleconnnections as discussed above [*Barreiro et al.*, 2005] and would have been exacerbated by the closing of the Panama Seaway in the early Pliocene, which caused the North Atlantic to warm, thereby restricting wintertime snowfall on continental North America [*Klocker et al.*, 2004]. In fact, continental climate conditions in the early Pliocene conformed to an El Niño-like pattern [*Molnar and Cane*, 2002] providing some verification, based on observations, that North American climate was influenced by low-latitude temperature patterns. Warmer winters, combined with summertime temperatures at least as warm as today, may be the reason why the growth of large North American ice sheets was inhibited until about 3.5 Ma [*Mudelsee and Raymo*, 2005] after upwelling regions began to cool. Cooling of upwelling regions alone could cause significant cooling of the continental interior of North America through atmospheric teleconnections [*Barreiro et al.*, 2005], thereby setting the stage for ice sheet growth.

[30] Warm upwelling regions may have also had an impact on the location and intensity of subtropical anticyclones and storm tracks, influencing seasonal rainfall on subtropical continents and the ocean and on meridional heat transport. The subtropical high-pressure anticyclones of the Pacific are a result mainly of land-sea temperature contrasts, with monsoon heating of the land and subsidence in the anticyclones. As such, subtropical highs are most intense in the summer when the air-sea contrast is most extreme. The cold water upwelling and equatorward advection that occurs at the eastern boundaries of the basin and the warm water poleward heat transport at the western boundaries generally cause a deepening of the high pressure in the east and an intensification of deep convection in the west [*Seager et al.*, 2003]. Thus in the early Pliocene, warmer upwelling regions, especially if accompanied by reduced poleward ocean heat transport expected during permanent El Niño-like conditions [*Hazeleger et al.*, 2004] and consistent with a deep thermocline [*Boccaletti et al.*, 2004; *Fedorov et al.*,

2004], may have caused the subtropical anticyclones to be broader and/or less intense, especially in the east.

[31] It is difficult to know what impact these inferred changes in subtropical pressure fields may have had on seasonal variability and storm tracks in the early Pliocene. However, we can begin to speculate for the North Pacific region based on recently observed decadal scale climate changes or the Pacific Decadal Oscillation (PDO) and the North Pacific Mode [*Barlow et al.*, 2001; *Mantua and Hare*, 2002]. Both modes explain significant variance in California coastal temperatures, and in the strength of the Aleutian Low and North Pacific High, especially in the northern and eastern Pacific. During the warm phases of the PDO, warmer California coastal SST, intensified Aleutian Low, and weakened North Pacific High, are associated with an increase in mean and kinetic energy in the middle and high latitudes (from 1980 to 2000) [*Hu et al.*, 2004]. The increase in energy indicates enhanced zonal flow as well as changes in eddy energy transfer, which could explain the observed increase of intense cyclones and anticyclones in recent decades [*Hu et al.*, 2004]. As such, we anticipate that warmer upwelling regions went hand-in-hand with changes in atmospheric energetics and regional precipitation patterns, but much work needs to be done to put our SST data into the proper context and to assess whether other factors dominate regional precipitation patterns. For example, greenhouse gas induced patterns of warming may cause a poleward shift in the storm tracks and precipitation [*Yin and Battisti*, 2001].

[32] The PDO can also provide insight into the link between winds, SST, and biological productivity. Since ~1950, SST along the California coast has increased by ~1°C. From the time of the 1977 shift to the warm phase of the PDO the thermocline along the California coast has deepened by 9–18 m and warmed by 0.6–1.3°C [*Palacios et al.*, 2004]. The deeper thermocline with a steeper temperature gradient serves as a barrier to the vertical transport of nutrients, which has had dramatic biological consequences, with decreases in phytoplankton, zooplankton, fish, and bird populations [*McGowan et al.*, 2003]. Observations over the last 50 years indicate that equatorward wind stress has increased [*Schwing and Mendelssohn*, 1997] due to the anthropogenic increase in greenhouse gas warming [*Bakun*, 1990]. In sum, although upwelling is occurring along the California coast, SSTs are relatively warm and productivity is low because as the thermocline has deepened; upwelled water is being derived from above the thermocline rather than from the nutrient rich cool water below the thermocline.

[33] The coupling between in SST and thermocline depth and the decoupling between upwelling strength, productivity, and SST that occur as part of the pattern of recent climate change highlight the importance of considering changes in subsurface conditions to understand early Pliocene climate and sustained warm climate conditions in general. Future Pliocene research will need to focus on improving productivity records with more specialized proxies and characterizing changes in the nutrient level and temperature of subsurface source waters to upwelling regions. Investigating the mechanisms that influenced the temperature and nutrient content of subsurface water during the Pliocene warm period may lead to better predictions of long-term changes in coastal productivity as the Earth warms in the future.

7. Conclusions

[34] The California margin, Peru margin, and the EEP were all significantly warmer during the early Pliocene compared to today. While zonal SST reconstructions are needed, thus far the data indicate that upwelling regions cooled dramatically through the Pliocene/Pleistocene transition. The decoupling between SST and productivity at our locations suggests that SST changes can not be explained by changes in the strength of upwelling favorable winds alone. Rather, even while SSTs were warm, some upwelling of nutrient enriched water must have occurred. When possible, more direct indicators of upwelling, such as the relative abundance of upwelling favoring diatom species used in the Benguela current [*Marlow et al.*, 2000], should be used to confirm that upwelling was occurring during the early Pliocene even as SST was warm in global upwelling regions. In addition, more detailed productivity proxies should be used at upwelling sites to asses changes in the type of productivity (e.g., coccolithophorid dominant versus diatom dominant), as these changes could impact the global carbon cycle by changing the relative burial of organic and inorganic carbon.

[35] Our records of SST and productivity, taken together with other records showing warmer SST in upwelling regions around the globe, support the theory of a deeper ventilated thermocline throughout the world's oceans during the warm Pliocene. To confirm this hypothesis and to further understand the mechanisms which caused a shoaling/cooling thermocline from the Pliocene to the Pleistocene, subsurface temperature records are needed from a variety of global locations. Subsurface temperature and nutrient records will also be needed to understand how the source of upwelling water changed through time either through changes in subsurface circulation or nutrient cycling.

[36] The cooling of the Earth's climate which culminated in the intense ice age cycles of the Pleistocene is reflected in a cooling SST trend at upwelling locations which began ~4 m.y. ago. The fact that upwelling regions began cooling before the onset of significant Northern Hemisphere glaciation indicates that high-latitude processes related to ice growth alone can not account for the cooling climate. Alternative explanations for global cooling through the Pliocene, such as feedbacks that involve changing SST in upwelling regions and a gradually shoaling thermocline, should be considered.

[37] **Acknowledgments.** We thank the anonymous reviewers whose comments helped us improve this manuscript. We also thank T. Herbert and K. Lawrence for helpful discussion. Analytical support was provided by R. Franks, and E. Green, M. Flower, and F. Mosqueda assisted in sample preparation and analysis. We thank the Ocean Drilling Program (ODP) for providing samples. This work was made possible through funding by the National Science Foundation (OCE-08 1697 to A.C.R and OCE-623419 to A.C.R) and a Center for the Dynamics and Evolution of the Land-Sea Interface (CDELSI) Ocean Health and Environmental Change Graduate Student Fellowship (to P.S.D).

References

Abe, C., M. Yamamoto, and T. Irino (2006), Organic carbon and biomarker variations, sites 1237 and 1239 [online], *Proc. Ocean Drill. Program Sci. Results*, *202*. (Available at http://www-odp.tamu.edu/publications/202_SR/203/203.htm)

Bakun, A. (1990), Global climate change and intensification of coastal ocean upwelling, *Science*, *247*, 198–201.

Bakun, A., and C. S. Nelson (1991), The seasonal cycle of wind-stress curl in subtropical eastern boundary current regions, *J. Phys. Oceanogr.*, *21*, 1815–1834.

Barlow, M., S. Nigam, and E. H. Berbery (2001), ENSO Pacific decadal variability, and U.S. summertime precipitation, drought, and stream flow, *J. Clim.*, *14*, 2105–2128.

Barreiro, M., S. G. Philander, and R. C. Pacanowski (2005), Simulations of warm tropical conditions with application to middle Pliocene atmospheres, *Clim. Dyn.*, *26*, 349–365.

Boccaletti, G., R. C. Pacanowski, S. G. Philander, and A. V. Federov (2004), The thermal structure of the upper ocean, *J. Phys. Oceanogr.*, *34*, 888–902.

Bryan, F. (1987), Parameter sensitivity of primary equation ocean general circulation models, *J. Phys. Oceanogr.*, *17*, 970–985.

Cane, M. A. (1986), El Niño, *Annu. Rev. Earth Planet. Sci.*, *14*, 43–70.

Cane, M. A., and P. Molnar (2001), Closing of the Indonesian Seaway as a precursor to East African aridification around 3–4 million years ago, *Nature*, *411*, 157–161.

Chaisson, W. P., and A. C. Ravelo (2000), Pliocene development of the east-west hydrographic gradient in the equatorial Pacific, *Paleoceanography*, *15*, 497–505.

Chun, C. O. J., and M. L. Delaney (2006), Phosphorus, barium, manganese, and uranium concentrations and geochemistry, Nazca Ridge Site 1237 sediments, *Proc. Ocean Drill. Program Sci. Results*, *202*, doi:10.2973/odp.proc.sr.202.205.2006.

Dekens, P. S., D. W. Lea, H. J. Spero, and D. K. Pak (2002), Core top calibration of Mg/Ca in tropical planktonic foraminifera: Refining paleotemperature estimation, *Geochem. Geophys. Geosyst.*, *3*(4), 1022, doi:10.1029/2001GC000200.

Delaney, M. L., and L. D. Anderson (2000), Data report: Phosphorus concentrations and geochemistry in California margin sediments, *Proc. Ocean Drill. Program Sci. Results*, *167*, 195–202.

Dowsett, H., J. Barron, and R. Poore (1996), Middle Pliocene sea surface temperatures: A global reconstruction, *Mar. Micropaleontol.*, *27*, 13–25.

Farrell, J. W., I. Raffi, T. R. Janecek, D. W. Murray, M. Levitan, K. A. Dadey, K.-C. Emeis, M. Lyle, J.-A. Flores, and S. Hovan (1995), Late Neogene sedimentation patterns in the eastern equatorial Pacific Ocean, *Proc. Ocean Drill. Program Sci. Results*, *138*, 289–319.

Fedorov, A. V., R. C. Pacanowski, S. G. Philander, and G. Boccaletti (2004), The effect of salinity on the wind-driven circulation and the thermal structure of the upper ocean, *J. Phys. Oceanogr.*, *34*, 1949–1966.

Federov, A. V., P. S. Dekens, M. McCarthy, A. C. Ravelo, P. B. deMenocal, M. Barreiro, R. C. Pacanowski, and S. G. Philander (2006), The Pliocene paradox (mechanisms for a permanent El Niño), *Science*, *312*, 1485–1489.

Groeneveld, J., S. Steph, R. Tiedemann, D. Garbe-Schonberg, D. Nurnberg, and A. Sturm (2006), Pliocene mixed-layer oceanography for Site 1241 using combined Mg/Ca and δ^{18}O analyses of *Globigerinoides sacculifer*, *Proc. Ocean Drill. Program Sci. Results*, *202*, doi:10.2973/odp.proc.sr.202.209.2006.

Harvey, H. R. (2000), Alteration processes of alkenones and related lipids in water columns and sediments, *Geochem. Geophys. Geosyst.*, *1*(8), doi:10.1029/2000GC000054.

Haug, G. H., and R. Tiedemann (1998), Effect of the formation of the Isthmus of Panama on Atlantic Ocean thermohaline circulation, *Nature*, *393, 673–676.*

Haug, G. H., D. M. Sigman, R. Tiedemann, T. F. Pedersen, and M. Sarnthein (1999), Onset of permanent stratification in the subarctic Pacific Ocean, *Nature*, *401*, 779–782.

Hazeleger, W., R. Seager, M. A. Cane, and N. H. Naik (2004), How can tropical Pacific Ocean heat transport vary, *J. Phys. Oceanogr.*, *34*, 320–333.

Herbert, T. D., and J. D. Schuffert (1998), Alkenone unsaturation estimates of late Miocene through late Pliocene sea-surface temperatures at Site 958, *Proc. Ocean Drill. Program Sci. Results*, *159T*, 17–21.

Hu, Q., Y. Tawaye, and S. Feng (2004), Variations of the Northern Hemisphere atmospheric energetics, *J. Clim.*, *17*, 1975–1986.

Klocker, A., M. Prange, and M. Schulz (2004), Testing the influence of the Central American Seaway on orbitally forced Northern Hemisphere glaciation, *Geophys. Res. Lett.*, *32*, L03703, doi:10.1029/2004GL021564.

Lampitt, R. S., E. Fahrbach, B. Schneider, R. R. Schneider, S. V. Smith, J. R. Toggweiler, A. J. Watson, and B. Zeitzschel (1995), Does upwelling have a significant influence on the global carbon cycle?, in *Upwelling in the Ocean, Modern Processes and Ancient Records*, *Environ. Sci. Res. Rep.*, vol. ES 18, edited by C. P. Summerhayes et al., pp. 383–404, John Wiley, Hoboken, N. J.

Lau, K.-M., and S. Shen (1988), On the dynamics of intraseasonal oscillations and ENSO, *J. Atmos. Sci.*, *45*, 1781–1797.

Lawrence, K. T., Z. Liu, and T. D. Herbert (2006), Evolution of the eastern tropical Pacific through Plio-Pleistocene glaciation, *Science*, *312*, 79–83.

Ledwell, J. R., A. J. Watson, and C. Law (1993), Evidence for slow mixing across the pycnocline from an open-ocean tracer-release experiment, *Nature*, *364*, 701–703.

Levitus, S., and T. P. Boyer (1994), *World Ocean Atlas 1994*, vol. 4, *Temperature, NOAA Atlas NESDIS*, vol. 4, 129 pp., NOAA., Silver Spring, Md.

Lyle, M., C. Koizumi, C. Richter, and the Shipboard Scientific Party (1997), *Proceedings of the Ocean Drilling Program Initial Results*, vol. 167, Ocean Drill. Program, College Station, Tex.

Mantua, N. J., and S. R. Hare (2002), The Pacific Decadal Oscillation, *J. Oceanogr.*, *58*, 35–44.

Marlow, F. R., C. B. Lange, G. Wefer, and A. Rosell-Mele (2000), Upwelling intensification as part of the Pliocene-Pleistocene climate transition, *Science*, *290*, 2288–2291.

Mayer, L. A., N. Pisias, and T. Janeck (1992), *Proceedings of the Ocean Drilling Program Initial Results*, vol. 138, Ocean Drill. Program, College Station, Tex.

McGowan, J. A., S. J. Bograd, R. J. Lynn, and A. J. Miller (2003), The biological response to the 1977 regime shift in the California Current, *Deep Sea Res., Part II*, *50*, 2567–2582.

Mendelssohn, R., and F. B. Schwing (2002), Common and uncommon trends in SST and wind stress in the California and Peru-Chile current systems, *Prog. Oceanogr.*, *53*, 141–162.

Mix, A. C., R. Tiedemann, and P. Blum (2003), *Proceedings of the Ocean Drilling Program Initial Results*, vol. 202, Ocean Drill. Program, College Station, Tex.

Molnar, P., and M. A. Cane (2002), El Niño's tropical climate and teleconnections as a blueprint for pre-Ice Age climates, *Paleoceanography*, *17*(2), 1021, doi:10.1029/2001PA000663.

Mudelsee, M., and M. E. Raymo (2005), Slow dynamics of the Northern Hemisphere glaciation, *Paleoceanography*, *20*, PA4022, doi:10.1029/2005PA001153.

Müller, P. J., G. Krist, G. Ruhland, I. von Storch, and A. Rosell-Melé (1998), Calibration of the alkenone paleotemperature index $U_{37}^{k'}$ based on core-tops from the eastern South Atlantic and the global ocean (60°N–60°S), *Geochim. Cosmochim. Acta*, *62*, 1757–1772.

Nürnberg, D., A. Muller, and R. R. Schneider (2000), Paleo-sea surface temperature calculations in the equatorial east Atlantic from Mg/Ca ratios in planktonic foraminifera: A comparison to sea surface estimates from $U_{37}^{k'}$, oxygen isotopes, and foraminiferal transfer functions, *Paleoceanography*, *15*, 124–134.

Okada, H., and S. Honjo (1973), The distribution of oceanic coccolithophorids in the Pacific, *Deep Sea Res.*, *20*, 355–374.

Palacios, D. M., S. J. Bograd, R. Mendelssohn, and F. B. Schwing (2004), Long-term and seasonal trends in stratification in the California Current, *J. Geophys. Res.*, *109*, C10016, doi:10.1029/2004JC002380.

Philander, S. G., and A. V. Fedorov (2003), Role of tropics in changing the response to Milankovitch forcing some three million years ago, *Paleoceanography*, *18*(2), 1045, doi:10.1029/2002PA000837.

Pollard, D. (2000), Comparisons of ice-sheet surface mass budgets from Paleoclimate Modeling Intercomparison Project (PMIP) simulations, *Global Planet. Change*, *24*, 79–106.

Prahl, F. G., L. A. Muehlhausen, and D. L. Zahnle (1988), Further evaluation of long-chain alkenones as indicators of paleooceanographic conditions, *Geochim. Cosmochim. Acta*, *52*, 2303–2310.

Prahl, F. G., G. J. de Lange, M. Lyle, and M. A. Sparrow (1989), Post-depositional stability of long-chain alkenones under contrasting redox conditions, *Nature*, *341*, 434–437.

Ravelo, A. C., and D. H. Andreasen (2000), Enhanced circulation during a warm period, *Geophys. Res. Lett.*, *27*(7), 1001–1004.

Ravelo, A. C., D. H. Andreasen, M. Lyle, A. Olivarez-Lyle, and M. W. Wara (2004), Regional climate shifts caused by gradual global cooling in the Pliocene epoch, *Nature*, *429*, 263–267.

Ravelo, A. C., P. S. Dekens, and M. D. McCarthy (2006), Evidence for El Niño-like conditions during the Pliocene, *GSA Today*, *16*, 4–11.

Rind, D. (1998), Latitudinal temperature gradients and climate change, *J. Geophys. Res.*, *103*, 5943–5972.

Roemmich, D., and J. McGowan (1995), Climatic warming and the decline of zooplankton in the California Current, *Science*, *267*, 1324–1326.

Schwing, F. B., and R. Mendelssohn (1997), Increased coastal upwelling in the California

Current System, *J. Geophys. Res.*, *102*, 3421–3438.

Schwing, F. B., T. Murphree, and P. M. Green (2002), The Northern Oscillation Index (NOI); a new climate index for the northeast Pacific, *Prog. Oceanogr.*, *53*, 115–139.

Seager, R., R. Murtugudde, N. Naik, A. Clement, N. Gordon, and J. Miller (2003), Air-sea interaction and the seasonal cycle of the subtropical anticyclones, *J. Clim.*, *16*, 1948–1966.

Shackleton, N. J., A. Berger, and W. R. Peltier (1990), An alternative astronomical calibration of the lower Pleistocene timescale based on ODP Site 677, *Trans. R. Soc. Edinburgh Earth Sci.*, *81*, 251–261.

Shackleton, N. J., S. Crowhurst, T. Hagelberg, N. G. Pisias, and D. A. Schneider (1995), A new late Neogene time scale: Application to leg 138 sites, *Proc. Ocean Drill. Program Sci. Results*, *138*, 73–101.

Snyder, M. A., L. C. Sloan, N. S. Diffenbaugh, and J. L. Bell (2003), Future climate change and upwelling in the California Current, *Geophys. Res. Lett.*, *30*(15), 1823, doi:10.1029/2003GL017647.

Villaneuva, J., J. A. Flores, and J. O. Grimalt (2002), A detailed comparison of the $U_{37}^{K'}$ and coccolith records over the past 290 kyears: Implications to the alkenone paleotemperature method, *Org. Geochem.*, *33*, 897–905.

Volkman, J. K. (2000), Ecological and environmental factors affecting alkenone distributions in seawater and sediments, *Geochem. Geophys. Geosyst.*, *1*(9), doi:10.1029/2000GC000061.

Wara, M. W., A. C. Ravelo, and M. L. Deleney (2005), Permanent El-Niño-like conditions during the Pliocene warm period, *Science*, *309*, 758–761.

Yin, J. H., and D. S. Battisti (2001), The importance of tropical sea surface temperature patterns in simulations of Last Glacial Maximum climate, *J. Clim.*, *14*, 565–581.

P. S. Dekens, M. D. McCarthy, and A. C. Ravelo, Ocean Sciences Department, University of California, Earth and Marine Science Building, A316, Santa Cruz, CA 95064, USA. (dekens@ucsc.edu)